A Multiscale Algorithm for Eddy-Current Nondestructive Evaluation Based On Volume-Integral Equations: Initial Concepts

R. Kim Murphy, Harold A. Sabbagh, and Elias H. Sabbagh

Victor Technologies, LLC
PO Box 7706, Bloomington, IN 47407-7706, USA
rkmurphy@att.net, has@sabbagh.com, ehs@sabbagh.com

Abstract **−** The use of coupled integral equations and anomalous currents allows us to efficiently remove 'background effects' in either forward or inverse modeling. This is especially true when computing the change in impedance due to a small flaw in the presence of a larger background anomaly. It is more accurate than simply computing the response with and without the flaw and then subtracting the two nearly equal values to obtain the small difference due to the flaw. In this paper, we compute the change in impedance of a probe due to a flaw in the presence of a much larger background anomaly, when the probe, which consists of a coil with a ferrite core, lies within the host region, and then apply the model and algorithm to the problem of inspecting a bolt hole in a plate or other layered medium with a 'SplitD' eddy-current probe.

Index Terms **−** Aircraft structures, computational, electromagnetics, eddy-current nondestructive evaluation, volume-integral equations.

I. INTRODUCTION

In [1] we developed a systematic procedure for analyzing problems in eddy-current nondestructive evaluation (NDE) by means of volume-integral equations (method of moments), and applied it to problems in aerospace, nuclear power, materials characterization, and other areas. One problem of interest to aerospace, and described in [1], is computing the response of a small crack located adjacent to a bolt hole. This requires the solution of a 'multiscale problem', with the bolt hole being the larger scale and the crack a much smaller scale. A method for solving this problem was developed using coupled integral equations, one for the anomalous currents within the bolt hole and the other for the anomalous currents within the crack. The algorithm was validated using measured data acquired by a 'conventional' surface coil scanned past the bolt hole and crack. By 'conventional' we mean that the coil was circular, with its axis normal to the surface of the host material, and containing no ferritic cores. The response of such coils can be computed analytically, as shown in [1]. That problem was chosen because of its relative simplicity in acquiring the data.

In this paper, we attack the more complicated, but common, problem in which inspections are performed by a complex probe positioned within the bolt hole. The probes typically used for inspections are complex, often of the 'SplitD' variety, with a transmit coil exciting the system, and two receive coils picking up the response. Furthermore, none of the three coils is circular, and they all enclose two ferritic cores, split longitudinally to give the 'SplitD' characteristic. See [1] for a description and application of these probes. This model then calls for three coupled integral equations, two as above, and the third for the probe.

We develop the 'probe-in-host' algorithm in Section II, and apply it to the SplitD probe problem in Section III. In order to keep the paper of reasonable length, we invite the reader to peruse [1] in order to get the background for understanding the terminology and concepts that are used throughout the paper. The development of the circuit response for the probe-in-host algorithm follows Chapter 5, 'Computing Network Immitance Functions from Field Calculations' of [1]. Also for length considerations, we have opted to discuss only the theoretical underpinnings of the algorithm. We will give a thorough presentation of **VIC-3D®** model results, as well as experimental validation in a second paper.

II. THE 'PROBE-IN-HOST' ALGORITHM

This algorithm is an extension of our multiscale background-removal algorithm. Both algorithms were developed to compute the change in impedance of a probe due to a flaw in a sample which also contains a much larger background anomaly. The background-removal algorithm addresses problems in which the flaw and background lie in one planar region, referred to as the 'host' region, and the probe, consisting of coil elements only, lies in a separate planar region. This permits the modeling of a coil scanned across the surface of a plate containing a bolt hole (the background) with an adjacent flaw.

The problem of modeling a probe containing a

Submitted On: October 4, 2015
Accepted On: February 25, 2016

ferrite core, and positioned within a bolt hole is addressed by the probe-in-host algorithm, which solves the more complex problem of a ferrite-cored probe that lies within the host region. The problem is illustrated in Fig. 1, but the algorithm is more general than shown, since the flaw may lie wholly or partially inside or outside the background, and this is true for the probe as well.

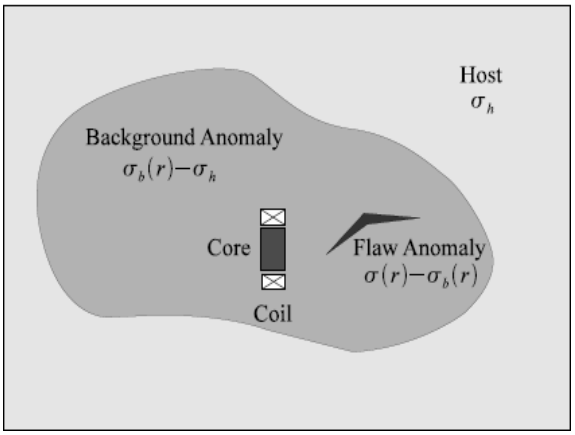

Fig. 1. The 'probe-in-background' problem. The conductivity within the host region is $\sigma(\mathbf{r})$. With background only (no flaw or probe) the conductivity is $\sigma_b(\mathbf{r})$. Outside the flaw (and probe), $\sigma(\mathbf{r}) = \sigma_b(\mathbf{r})$. Outside the background $\sigma(\mathbf{r}) = \sigma_b(\mathbf{r}) = \sigma_h$.

The conductivity at all points within the host region is given by $\sigma(\mathbf{r})$. For the corresponding unflawed problem with background and probe only, the function is $\sigma_u(\mathbf{r})$. Thus $\sigma(\mathbf{r})$ agrees with $\sigma_u(\mathbf{r})$ at all points outside the flaw. For the corresponding unflawed problem with background only (i.e., probe removed), the function is $\sigma_b(\mathbf{r})$. Thus, $\sigma_u(\mathbf{r})$ agrees with $\sigma_b(\mathbf{r})$ at all points outside probe. The conductivity of the host region has a uniform value of σ_h outside the background and flaw, where $\sigma(\mathbf{r}) = \sigma_u(\mathbf{r}) = \sigma_b(\mathbf{r}) = \sigma_h$. Finally, the permeabilities $\mu(\mathbf{r})$, $\mu_u(\mathbf{r})$, $\mu_b(\mathbf{r})$ and μ_h are defined analogously, and hence obey analogous relations.

Perhaps it would be more clear to think of building up to $\sigma(\mathbf{r})$ and $\mu(\mathbf{r})$ as follows: Start with the uniform conductivity and permeability, σ_h and μ_h of the host. Add the background to get $\sigma_b(\mathbf{r})$ and $\mu_b(\mathbf{r})$. Add the probe to get $\sigma_u(\mathbf{r})$ and $\mu_u(\mathbf{r})$. Finally, add the flaw to get $\sigma(\mathbf{r})$ and $\mu(\mathbf{r})$.

The anomalous current and magnetization, $\mathbf{J}_a(\mathbf{r})$ and $\mathbf{M}_a(\mathbf{r})$ respectively, satisfy the equations:

$$\mathbf{J}_a(\mathbf{r}) = (\sigma(\mathbf{r}) - \sigma_h)\mathbf{E}(\mathbf{r}), \tag{1}$$

$$\mathbf{M}_a(\mathbf{r}) = \left(\frac{1}{\mu_h} - \frac{1}{\mu(\mathbf{r})}\right)\mathbf{B}(\mathbf{r}), \tag{2}$$

where

$$\mathbf{E}(\mathbf{r}) = \mathbf{E}^{(i)}(\mathbf{r}) + \mathbf{E}(\mathbf{r})[J_a] + \mathbf{E}(\mathbf{r})[M_a], \tag{3}$$

$$\mathbf{B}(\mathbf{r}) = \mathbf{B}^{(i)}(\mathbf{r}) + \mathbf{B}(\mathbf{r})[J_a] + \mathbf{B}(\mathbf{r})[M_a], \tag{4}$$

and $\mathbf{E}^{(i)}(\mathbf{r})$ and $\mathbf{B}^{(i)}(\mathbf{r})$ are the incident electric and magnetic fields of the probe coil. Functionals, such as $\mathbf{E}(\mathbf{r})[\cdot]$ and $\mathbf{B}(\mathbf{r})[\cdot]$, are volume integrals with Green's function kernels.

We rewrite the right hand side of (1) and (2) as follows:

$$\begin{aligned}\mathbf{J}_a(\mathbf{r}) = {} & (\sigma_b(\mathbf{r}) - \sigma_h)\mathbf{E}(\mathbf{r}) \\ & + \big(\sigma_u(\mathbf{r}) - \sigma_b(\mathbf{r})\big)\mathbf{E}(\mathbf{r}) \\ & + \big(\sigma(\mathbf{r}) - \sigma_u(\mathbf{r})\big)\mathbf{E}(\mathbf{r}),\end{aligned} \tag{5}$$

$$\begin{aligned}\mathbf{M}_a(\mathbf{r}) = {} & \left(\frac{1}{\mu_h} - \frac{1}{\mu_b(\mathbf{r})}\right)\mathbf{B}(\mathbf{r}) \\ & + \left(\frac{1}{\mu_b(\mathbf{r})} - \frac{1}{\mu_u(\mathbf{r})}\right)\mathbf{B}(\mathbf{r}) \\ & + \left(\frac{1}{\mu_u(\mathbf{r})} - \frac{1}{\mu(\mathbf{r})}\right)\mathbf{B}(\mathbf{r}).\end{aligned} \tag{6}$$

Now notice that if we find solutions $\mathbf{J}_b(\mathbf{r})$, $\mathbf{J}_c(\mathbf{r})$, $\mathbf{J}_f(\mathbf{r})$, $\mathbf{M}_b(\mathbf{r})$, $\mathbf{M}_c(\mathbf{r})$, $\mathbf{M}_f(\mathbf{r})$ to the coupled equations,

$$\mathbf{J}_b(\mathbf{r}) = (\sigma_b(\mathbf{r}) - \sigma_h)\mathbf{E}(\mathbf{r}), \tag{7}$$

$$\mathbf{J}_c(\mathbf{r}) = \big(\sigma_u(\mathbf{r}) - \sigma_b(\mathbf{r})\big)\mathbf{E}(\mathbf{r}), \tag{8}$$

$$\mathbf{J}_f(\mathbf{r}) = \big(\sigma(\mathbf{r}) - \sigma_u(\mathbf{r})\big)\mathbf{E}(\mathbf{r}), \tag{9}$$

$$\mathbf{M}_b(\mathbf{r}) = \left(\frac{1}{\mu_h} - \frac{1}{\mu_b(\mathbf{r})}\right)\mathbf{B}(\mathbf{r}), \tag{10}$$

$$\mathbf{M}_c(\mathbf{r}) = \left(\frac{1}{\mu_b(\mathbf{r})} - \frac{1}{\mu_u(\mathbf{r})}\right)\mathbf{B}(\mathbf{r}), \tag{11}$$

$$\mathbf{M}_f(\mathbf{r}) = \left(\frac{1}{\mu_u(\mathbf{r})} - \frac{1}{\mu(\mathbf{r})}\right)\mathbf{B}(\mathbf{r}), \tag{12}$$

where

$$\begin{aligned}\mathbf{E}(\mathbf{r}) = {} & \mathbf{E}^{(i)}(\mathbf{r}) + \mathbf{E}(\mathbf{r})[J_b] + \mathbf{E}(\mathbf{r})[J_c] \\ & + \mathbf{E}(\mathbf{r})\big[J_f\big] + \mathbf{E}(\mathbf{r})[M_b] + \mathbf{E}(\mathbf{r})[M_c] \\ & + \mathbf{E}(\mathbf{r})\big[M_f\big],\end{aligned} \tag{13}$$

$$\begin{aligned}\mathbf{B}(\mathbf{r}) = {} & \mathbf{B}^{(i)}(\mathbf{r}) + \mathbf{B}(\mathbf{r})[J_b] + \mathbf{B}(\mathbf{r})[J_c] \\ & + \mathbf{B}(\mathbf{r})\big[J_f\big] + \mathbf{B}(\mathbf{r})[M_b] + \mathbf{B}(\mathbf{r})[M_c] \\ & + \mathbf{B}(\mathbf{r})\big[M_f\big],\end{aligned} \tag{14}$$

then the sums $\mathbf{J}_a(\mathbf{r}) = \mathbf{J}_b(\mathbf{r}) + \mathbf{J}_c(\mathbf{r}) + \mathbf{J}_f(\mathbf{r})$ and $\mathbf{M}_a(\mathbf{r}) = \mathbf{M}_b(\mathbf{r}) + \mathbf{M}_c(\mathbf{r}) + \mathbf{M}_f(\mathbf{r})$ satisfy (1) and (2).

Noting from (7-12) that $\mathbf{J}_b(\mathbf{r})$ and $\mathbf{M}_b(\mathbf{r})$ are zero outside the background, $\mathbf{J}_c(\mathbf{r})$ and $\mathbf{M}_c(\mathbf{r})$ are zero outside the probe core, and $\mathbf{J}_f(\mathbf{r})$ and $\mathbf{M}_f(\mathbf{r})$ are zero outside the flaw, we identify these anomalous currents and magnetizations as those of the background, probe core and flaw, respectively.

Since we will be solving for $\mathbf{J}_c(\mathbf{r})$ and $\mathbf{M}_c(\mathbf{r})$ only within the space occupied by the probe core, and the flaw does not intrude into that space, we can replace $\sigma_u(\mathbf{r})$ and $\mu_u(\mathbf{r})$ by $\sigma(\mathbf{r})$ and $\mu(\mathbf{r})$ in (8) and (11), respectively. Similarly, since we will be solving for $\mathbf{J}_f(\mathbf{r})$ and $\mathbf{M}_f(\mathbf{r})$ only within the space occupied by the flaw, and the probe

does not intrude into that space, we can replace $\sigma_u(\mathbf{r})$ and $\mu_u(\mathbf{r})$ by $\sigma_b(\mathbf{r})$ and $\mu_b(\mathbf{r})$ in (9) and (12), respectively.

With these substitutions, and in preparation for discretization, we reorder (7-12) as well as their unknowns, and rewrite them in the form:

$$\begin{aligned}\mathbf{E}^{(i)}(\mathbf{r}) = {} & \frac{1}{\sigma_b(\mathbf{r})-\sigma_h}\mathbf{J}_b(\mathbf{r}) - \mathbf{E}(\mathbf{r})[J_b] \\ & - \mathbf{E}(\mathbf{r})[M_b] - \mathbf{E}(\mathbf{r})[J_c] \\ & - \mathbf{E}(\mathbf{r})[M_c] - \mathbf{E}(\mathbf{r})\big[J_f\big] \\ & - \mathbf{E}(\mathbf{r})\big[M_f\big], \end{aligned} \tag{15}$$

$$\begin{aligned}\mathbf{B}^{(i)}(\mathbf{r}) = {} & -\mathbf{B}(\mathbf{r})[J_b] + \frac{\mu_b(\mathbf{r})\mu_h}{\mu_b(\mathbf{r})-\mu_h}\mathbf{M}_b(\mathbf{r}) \\ & - \mathbf{B}(\mathbf{r})[M_b] - \mathbf{B}(\mathbf{r})[J_c] \\ & - \mathbf{B}(\mathbf{r})[M_c] - \mathbf{B}(\mathbf{r})\big[J_f\big] \\ & - \mathbf{B}(\mathbf{r})\big[M_f\big], \end{aligned} \tag{16}$$

$$\begin{aligned}\mathbf{E}^{(i)}(\mathbf{r}) = {} & -\mathbf{E}(\mathbf{r})[J_b] - \mathbf{E}(\mathbf{r})[M_b] \\ & + \frac{1}{\sigma(\mathbf{r})-\sigma_b(\mathbf{r})}\mathbf{J}_c(\mathbf{r}) - \mathbf{E}(\mathbf{r})[J_c] \\ & - \mathbf{E}(\mathbf{r})[M_c] - \mathbf{E}(\mathbf{r})\big[J_f\big] \\ & - \mathbf{E}(\mathbf{r})\big[M_f\big], \end{aligned} \tag{17}$$

$$\begin{aligned}\mathbf{B}^{(i)}(\mathbf{r}) = {} & -\mathbf{B}(\mathbf{r})[J_b] - \mathbf{B}(\mathbf{r})[M_b] \\ & - \mathbf{B}(\mathbf{r})[J_c] + \frac{\mu(\mathbf{r})\mu_b(\mathbf{r})}{\mu(\mathbf{r})-\mu_b(\mathbf{r})}\mathbf{M}_c(\mathbf{r}) \\ & - \mathbf{B}(\mathbf{r})[M_c] - \mathbf{B}(\mathbf{r})\big[J_f\big] \\ & - \mathbf{B}(\mathbf{r})\big[M_f\big], \end{aligned} \tag{18}$$

$$\begin{aligned}\mathbf{E}^{(i)}(\mathbf{r}) = {} & -\mathbf{E}(\mathbf{r})[J_b] - \mathbf{E}(\mathbf{r})[M_b] \\ & - \mathbf{E}(\mathbf{r})[J_c] - \mathbf{E}(\mathbf{r})[M_c] \\ & + \frac{1}{\sigma(\mathbf{r})-\sigma_b(\mathbf{r})}\mathbf{J}_f(\mathbf{r}) - \mathbf{E}(\mathbf{r})\big[J_f\big] \\ & - \mathbf{E}(\mathbf{r})\big[M_f\big], \end{aligned} \tag{19}$$

$$\begin{aligned}\mathbf{B}^{(i)}(\mathbf{r}) = {} & -\mathbf{B}(\mathbf{r})[J_b] - \mathbf{B}(\mathbf{r})[M_b] \\ & - \mathbf{B}(\mathbf{r})[J_c] - \mathbf{B}(\mathbf{r})[M_c] \\ & - \mathbf{B}(\mathbf{r})\big[J_f\big] + \frac{\mu(\mathbf{r})\mu_b(\mathbf{r})}{\mu(\mathbf{r})-\mu_b(\mathbf{r})}\mathbf{M}_f(\mathbf{r}) \\ & - \mathbf{B}(\mathbf{r})\big[M_f\big]. \end{aligned} \tag{20}$$

Note that $\sigma_b(\mathbf{r}) = \sigma_h$ and $\mu_b(\mathbf{r}) = \mu_h$ in (17) and (18) for parts of the probe that lie outside the background, and in (19) and (20) for parts of the flaw that lie outside the background.

We will discretize these equations using three grids: a core grid, a coarse 'background' grid, and a fine 'flaw' grid. First we expand $\mathbf{J}_b(\mathbf{r})$, $\mathbf{J}_c(\mathbf{r})$ and $\mathbf{J}_f(\mathbf{r})$ in tent functions, and $\mathbf{M}_b(\mathbf{r})$, $\mathbf{M}_c(\mathbf{r})$ and $\mathbf{M}_f(\mathbf{r})$ in edge-elements, defined on the background, core and flaw grids, respectively. Then we use these same functions to test our equations. We multiply the equations by these functions, which have compact support spanning one or two grid cells along each direction, and integrate over space. We test (15), (17), and (19) with the tent functions, and (16), (18), and (20) with the edge-elements, defined on the background, core and flaw grids respectively. This gives the discretized matrix equation:

$$\begin{bmatrix} \mathbf{A}_{bb}^{(ee)} & -\mathbf{G}_{bb}^{(em)} & -\mathbf{G}_{bc}^{(ee)} & -\mathbf{G}_{bc}^{(em)} \\ -\mathbf{G}_{bb}^{(me)} & \mathbf{A}_{bb}^{(mm)} & -\mathbf{G}_{bc}^{(me)} & -\mathbf{G}_{bc}^{(mm)} \\ -\mathbf{G}_{cb}^{(ee)} & -\mathbf{G}_{cb}^{(em)} & \mathbf{A}_{cc}^{(ee)} & -\mathbf{G}_{cc}^{(em)} \\ -\mathbf{G}_{cb}^{(me)} & -\mathbf{G}_{cb}^{(mm)} & -\mathbf{G}_{cc}^{(me)} & \mathbf{A}_{cc}^{(mm)} \\ -\mathbf{G}_{fb}^{(ee)} & -\mathbf{G}_{fb}^{(em)} & -\mathbf{G}_{fc}^{(ee)} & -\mathbf{G}_{fc}^{(em)} \\ -\mathbf{G}_{fb}^{(me)} & -\mathbf{G}_{fb}^{(mm)} & -\mathbf{G}_{fc}^{(me)} & -\mathbf{G}_{fc}^{(mm)} \end{bmatrix} \begin{bmatrix} -\mathbf{G}_{bf}^{(ee)} & -\mathbf{G}_{bf}^{(em)} \\ -\mathbf{G}_{bf}^{(me)} & -\mathbf{G}_{bf}^{(mm)} \\ -\mathbf{G}_{cf}^{(ee)} & -\mathbf{G}_{cf}^{(em)} \\ -\mathbf{G}_{cf}^{(me)} & -\mathbf{G}_{cf}^{(mm)} \\ \mathbf{A}_{ff}^{(ee)} & -\mathbf{G}_{ff}^{(em)} \\ -\mathbf{G}_{ff}^{(me)} & \mathbf{A}_{ff}^{(mm)} \end{bmatrix} \begin{bmatrix} \mathbf{J}_b \\ \mathbf{M}_b \\ \mathbf{J}_c \\ \mathbf{M}_c \\ \mathbf{J}_f \\ \mathbf{M}_f \end{bmatrix} = \begin{bmatrix} \mathbf{E}_b^{(i)} \\ \mathbf{B}_b^{(i)} \\ \mathbf{E}_c^{(i)} \\ \mathbf{B}_c^{(i)} \\ \mathbf{E}_f^{(i)} \\ \mathbf{B}_f^{(i)} \end{bmatrix}, \tag{21}$$

which we solve for the vectors $\mathbf{J}_b$, $\mathbf{J}_c$ and $\mathbf{J}_f$ of expansion coefficients for the anomalous currents, and the vectors $\mathbf{M}_b$, $\mathbf{M}_c$ and $\mathbf{M}_f$ of expansion coefficients for the anomalous magnetizations, of the background, probe core and flaw respectively. Here, $\mathbf{A} = \mathbf{Q} - \mathbf{G}$, where the matrix $\mathbf{Q}$ contains the dependence on the anomalous electromagnetic material properties of the probe core, background and flaw.

III. THE PROBE-IN-BACKGROUND PROBLEM

Now we consider the simple case in which: 1) The permeability of the background, flaw and host are the same, and 2) The probe lies within the background and has the same conductivity as the background. From (10) and (12) we see that the first condition implies $\mathbf{M}_b = \mathbf{M}_f = 0$, and from (8) the second condition implies that $\mathbf{J}_c = 0$. Then the field equations (15-20) reduce to the three equations,

$$\begin{aligned}\mathbf{E}^{(i)}(\mathbf{r}) = {} & \frac{1}{\sigma_b(\mathbf{r})-\sigma_h}\mathbf{J}_b(\mathbf{r}) - \mathbf{E}(\mathbf{r})[J_b] \\ & - \mathbf{E}(\mathbf{r})[M_c] - \mathbf{E}(\mathbf{r})\big[J_f\big], \end{aligned} \tag{22}$$

$$\begin{aligned}\mathbf{B}^{(i)}(\mathbf{r}) = {} & -\mathbf{B}(\mathbf{r})[J_b] + \frac{\mu(\mathbf{r})\mu_h}{\mu(\mathbf{r})-\mu_h}\mathbf{M}_c(\mathbf{r}) \\ & -\mathbf{B}(\mathbf{r})[M_c] - \mathbf{B}(\mathbf{r})\big[J_f\big], \end{aligned} \tag{23}$$

$$\begin{aligned}\mathbf{E}^{(i)}(\mathbf{r}) = {} & -\mathbf{E}(\mathbf{r})[J_b] - \mathbf{E}(\mathbf{r})[M_c] \\ & + \frac{1}{\sigma(\mathbf{r})-\sigma_b(\mathbf{r})}\mathbf{J}_f(\mathbf{r}) - \mathbf{E}(\mathbf{r})\big[J_f\big], \end{aligned} \tag{24}$$

and the discretized matrix equation reduces to:

$$\begin{bmatrix} [\mathbf{Q}_{bb}^{(ee)} - \mathbf{G}_{bb}^{(ee)}] & -\mathbf{G}_{bc}^{(em)} & -\mathbf{G}_{bf}^{(ee)} \\ -\mathbf{G}_{cb}^{(me)} & [\mathbf{Q}_{cc}^{(mm)} - \mathbf{G}_{cc}^{(mm)}] & -\mathbf{G}_{cf}^{(me)} \\ -\mathbf{G}_{fb}^{(ee)} & -\mathbf{G}_{fc}^{(em)} & [\mathbf{Q}_{ff}^{(ee)} - \mathbf{G}_{ff}^{(ee)}] \end{bmatrix} \begin{bmatrix} \mathbf{J}_b \\ \mathbf{M}_c \\ \mathbf{J}_f \end{bmatrix} = \begin{bmatrix} \mathbf{E}_b^{(i)} \\ \mathbf{B}_c^{(i)} \\ \mathbf{E}_f^{(i)} \end{bmatrix}. \quad (25)$$

We recast this matrix equation in the form of the three coupled equation:

$$[\mathbf{Q}_{cc}^{(mm)} - \mathbf{G}_{cc}^{(mm)}]\mathbf{M}_c = \mathbf{B}_c^{(i)} + \mathbf{G}_{cb}^{(me)}\mathbf{J}_b + \mathbf{G}_{cf}^{(me)}\mathbf{J}_f, \quad (26)$$

$$[\mathbf{Q}_{bb}^{(ee)} - \mathbf{G}_{bb}^{(ee)}]\mathbf{J}_b = \mathbf{E}_b^{(i)} + \mathbf{G}_{bc}^{(em)}\mathbf{M}_c + \mathbf{G}_{bf}^{(ee)}\mathbf{J}_f, \quad (27)$$

$$[\mathbf{Q}_{ff}^{(ee)} - \mathbf{G}_{ff}^{(ee)}]\mathbf{J}_f = \mathbf{E}_f^{(i)} + \mathbf{G}_{fb}^{(ee)}\mathbf{J}_b + \mathbf{G}_{fc}^{(em)}\mathbf{M}_c. \quad (28)$$

If the grids for the probe core, background and flaw are evenly spaced along the *x*, *y*, and *z* directions, then the **G** matrices that appear on the left-hand side of these equations have a Toeplitz/Hankel structure. This, along with the sparse nature of the **Q** matrices, allows the matrix multiplications on the left-hand side of the equations to be performed quickly. Therefore, for a given value of the right-hand side, the equations can be solved efficiently using a conjugate-gradient matrix equation solver. The **G** matrices on the right-hand side of the equations lack this structure, so evaluation of the right-hand side is much more computationally expensive.

We start with initial values of zero for $\mathbf{M}_c$, $\mathbf{J}_b$, and $\mathbf{J}_f$ and cycle through the equations, updating the right-hand sides and solving for updated unknowns until changes in the magnetizations and currents are insignificant.

For small flaws, $\mathbf{J}_f$ will have little effect on $\mathbf{M}_c$ and $\mathbf{J}_b$. In this case, we can set $\mathbf{J}_f = 0$ in (26) and (27), and cycle through these equations to solve for $\mathbf{M}_c$ and $\mathbf{J}_b$, which amounts to solving the unflawed problem. Then, we insert these values into (28) and solve for $\mathbf{J}_f$. Experimental evidence supports this 'small flaw' approximation for flaws typical in nondestructive evaluation.

IV. BOLT-HOLE INSPECTION WITH THE SPLITD PROBE

We now consider the problem of inspecting a bolt hole in a plate or other layered planar medium with the 'SplitD' probe that is depicted in Fig. 2.

The probe is pulled along the direction of the bolt hole axis while it is spinning in the circumferential direction, thereby generating a two-dimensional raster scan. This is an important problem in the aircraft industry, and led to the development of this probe. The probe comprises a racetrack driver coil in combination with a pickup coil wound in a differential configuration around a 'SplitD' ferrite core. See pages 81-91 of [1] for a description of such a probe, with examples of its use in characterizing surface cracks within bolt holes in a benchmark test case.

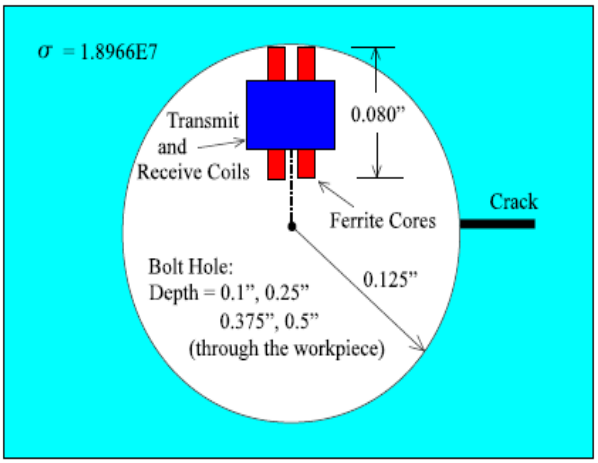

Fig. 2. Illustrating the SplitD probe within the bolt hole. The probe is spun about the axis of the bolt hole (out of page).

We compute the change in the pickup impedance due to the flaw. The corresponding circuit diagram is shown in Fig. 3. The ferrite core has the effect of increasing the inductances, L_d and L_p, of the driver and pickup coils. We model this effect with additional coil turns represented in the figure by L_μ and L_μ, respectively. Setting the sum of the voltage drops around each of the circuits for driver coil with core, pickup coil with core, background and flaw to zero gives:

$$V_1(\alpha) = (Z_{dd} + Z_{d\mu} + Z_{\mu d} + Z_{\mu\mu})I_1 + (Z_{dp} + Z_{d\mu'} + Z_{\mu p} + Z_{\mu\mu'})I_2(\alpha) + (Z_{d3} + Z_{\mu 3})I_3(\alpha) + \alpha(Z_{d4} + Z_{\mu 4})I_4, \quad (29)$$

$$V_2(\alpha) = (Z_{pd} + Z_{p\mu} + Z_{\mu' d} + Z_{\mu' \mu})I_1 + (Z_{pp} + Z_{p\mu'} + Z_{\mu' p} + Z_{\mu'\mu'})I_2(\alpha) + (Z_{p3} + Z_{\mu' 3})I_3(\alpha) + \alpha(Z_{p4} + Z_{\mu' 4})I_4, \quad (30)$$

$$0 = (Z_{3d} + Z_{3\mu})I_1 + (Z_{3p} + Z_{3\mu'})I_2(\alpha) + Z_{33}I_3(\alpha) + \alpha Z_{34}I_4, \quad (31)$$

$$0 = (Z_{4d} + Z_{4\mu})I_1 + (Z_{4p} + Z_{4\mu'})I_2(1) + Z_{43}I_3(1) + Z_{44}I_4. \quad (32)$$

The equations are parameterized by α, which has a value of unity for the problem we are solving, which includes a flaw, and a value of zero for the corresponding unflawed problem. Since the flaw current, I_4, is zero when $\alpha = 0$, we write it as αI_4.

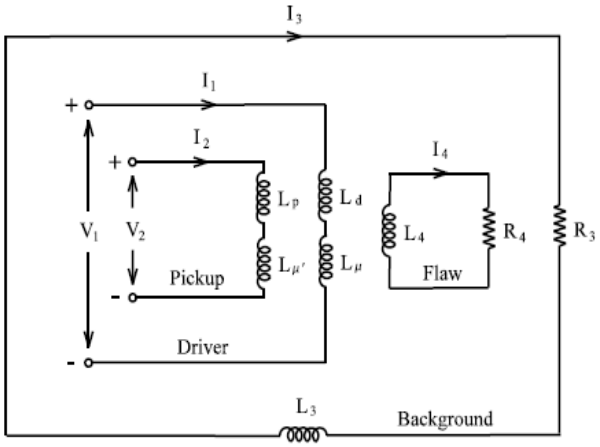

Fig. 3. Equivalent circuit diagram for the probe-in-background problem with the SplitD probe. L_d and L_p are the inductances of the driver and pickup coils. L_μ and L_μ, model the increased inductance due to the ferrite core.

The current I_2 in the pickup coil will be very small (theoretically zero), so we will ignore the terms in (29-32) that involve I_2. And we will combine L_d and L_μ into a single inductance, L_1, and L_p and L_μ, into a single inductance, L_2. The circuit equations then become:

$$V_1(\alpha) = Z_{11}I_1 + Z_{13}I_3(\alpha) + \alpha Z_{14}I_4, \quad (33)$$
$$V_2(\alpha) = Z_{21}I_1 + Z_{23}I_3(\alpha) + \alpha Z_{24}I_4, \quad (34)$$
$$0 = Z_{31}I_1 + Z_{33}I_3(\alpha) + \alpha Z_{34}I_4, \quad (35)$$
$$0 = Z_{41}I_1 + Z_{43}I_3(1) + Z_{44}I_4, \quad (36)$$

where

$$\begin{aligned} Z_{11} &= Z_{dd} + Z_{d\mu} + Z_{\mu d} + Z_{\mu\mu} \\ Z_{21} &= Z_{pd} + Z_{p\mu} + Z_{\mu' d} + Z_{\mu'\mu} \\ Z_{1j} &= Z_{dj} + Z_{\mu j} \\ Z_{i1} &= Z_{id} + Z_{i\mu} \\ Z_{2j} &= Z_{pj} + Z_{\mu' j}. \end{aligned} \quad (37)$$

Solving (35) for I_3 when $\alpha = 0$ (no flaw) gives:

$$I_3(0) = -\frac{Z_{31}}{Z_{33}} I_1, \quad (38)$$

and solving (35) and (36) for $\alpha = 1$ (with flaw) gives

$$I_3(1) = -\frac{\begin{vmatrix} Z_{31} & Z_{34} \\ Z_{41} & Z_{44} \end{vmatrix}}{\begin{vmatrix} Z_{33} & Z_{34} \\ Z_{43} & Z_{44} \end{vmatrix}} I_1, \quad (39)$$

$$I_4 = -\frac{\begin{vmatrix} Z_{33} & Z_{31} \\ Z_{43} & Z_{41} \end{vmatrix}}{\begin{vmatrix} Z_{33} & Z_{34} \\ Z_{43} & Z_{44} \end{vmatrix}} I_1. \quad (40)$$

Equations (38-40) give the distributed currents for the background and flaw in terms of the driver current I_1. Putting these into (34) gives the pickup voltage without and with the flaw:

$$V_2(0) = \left(Z_{21} - Z_{23}\frac{Z_{31}}{Z_{33}}\right) I_1, \quad (41)$$

$$V_2(1) = \left(Z_{21} - Z_{23}\frac{\begin{vmatrix} Z_{31} & Z_{34} \\ Z_{41} & Z_{44} \end{vmatrix}}{\begin{vmatrix} Z_{33} & Z_{34} \\ Z_{43} & Z_{44} \end{vmatrix}} - Z_{24}\frac{\begin{vmatrix} Z_{33} & Z_{31} \\ Z_{43} & Z_{44} \end{vmatrix}}{\begin{vmatrix} Z_{33} & Z_{34} \\ Z_{43} & Z_{44} \end{vmatrix}} \right) I_1. \quad (42)$$

The change in the transfer impedance due to the flaw is thus,

$$\begin{aligned} dZ_{21} &= \frac{V_2(1)}{I_1} - \frac{V_2(0)}{I_1} \\ &= -\left(Z_{23}\frac{\begin{vmatrix} Z_{31} & Z_{34} \\ Z_{41} & Z_{44} \end{vmatrix}}{\begin{vmatrix} Z_{33} & Z_{34} \\ Z_{43} & Z_{44} \end{vmatrix}} + Z_{24}\frac{\begin{vmatrix} Z_{33} & Z_{31} \\ Z_{43} & Z_{44} \end{vmatrix}}{\begin{vmatrix} Z_{33} & Z_{34} \\ Z_{43} & Z_{44} \end{vmatrix}} - Z_{23}\frac{Z_{31}}{Z_{33}} \right). \end{aligned} \quad (43)$$

We now re-solve the equations in a form more useful for the calculation of dZ_{21}. From (35) the background current is:

$$I_3(\alpha) = -\left(\frac{Z_{31}}{Z_{33}} I_1 + \alpha \frac{Z_{34}}{Z_{33}} I_4\right), \quad (44)$$

and putting this result into (34) we get:

$$\begin{aligned} V_2(\alpha) &= Z_{21}I_1 - \frac{Z_{23}}{Z_{33}}(Z_{31}I_1 + \alpha Z_{34}I_4) + \alpha Z_{24}I_4 \\ &= \left(Z_{21} - \frac{Z_{23}Z_{31}}{Z_{33}}\right) I_1 \\ &\quad + \alpha\left(Z_{24} - \frac{Z_{23}Z_{34}}{Z_{33}}\right) I_4. \end{aligned} \quad (45)$$

The first terms in the two parentheses represent the direct coupling of the pickup to the driver and the flaw. The second terms represent the coupling, through the background, of the pickup to the driver and the flaw. The background produces a field that opposes that due to the direct coupling, thus reducing the impedance.

To find the voltage produced at the flaw by a current flowing through the pickup coil, we need to add the terms from I_2 to (35) and (36), which we rewrite as:

$$0 = Z_{31}I_1 + Z_{32}I_2(1) + Z_{33}I_3(1) + Z_{34}I_4, \quad (46)$$
$$0 = Z_{41}I_1 + Z_{42}I_2(1) + Z_{43}I_3(1) + Z_{44}I_4. \quad (47)$$

Solving (46) for I_3 gives:

$$I_3(1) = -\frac{1}{Z_{33}}(Z_{31}I_1 + Z_{32}I_2(1) + Z_{34}I_4), \quad (48)$$

and putting this into (47) gives:

$$\begin{aligned} 0 &= \left(Z_{41} - \frac{Z_{43}Z_{31}}{Z_{33}}\right) I_1 + \left(Z_{42} - \frac{Z_{43}Z_{32}}{Z_{33}}\right) I_2 \\ &\quad + \left(Z_{44} - \frac{Z_{43}Z_{34}}{Z_{33}}\right) I_4. \end{aligned} \quad (49)$$

The second term of (49) gives the voltage across the flaw due to the pickup current, and includes the coupling through the background as well as the direct coupling.

Now we evaluate the voltage across the pickup coil due to the flaw in terms of field quantities, for the purpose of computation. From (45) we have:

$$V_2(1) - V_2(0) = \left(Z_{24} - \frac{Z_{23}Z_{34}}{Z_{33}}\right) I_4. \qquad (50)$$

This is equal to the line integral around the pickup coil,

$$dV_2 = -\int_{coil} \mathbf{E}^{(4)}(\mathbf{r}) \cdot \mathbf{dl}, \qquad (51)$$

where $\mathbf{E}^{(4)}(\mathbf{r})$ is the field produced at the pickup coil by the flaw current I_4. We rewrite this as:

$$dV_2 = \frac{-\int_{coil} \mathbf{E}^{(4)}(\mathbf{r}) \cdot I_2(1)\mathbf{dl}}{I_2(1)} = \frac{-\int_{coil} \mathbf{E}^{(4)}(\mathbf{r}) \cdot \mathbf{J}^{(2)}(\mathbf{r})dV}{I_2(1)}, \qquad (52)$$

where the volume integral in the last expression is the integral over the coil volume of the dot product of the field, $\mathbf{E}^{(4)}(\mathbf{r})$, at the pickup coil due to the flaw with the current density, $\mathbf{J}^{(2)}(\mathbf{r})$, of the pickup current.

Now by the reciprocity theorem we have the symmetry:

$$\int_{coil} \mathbf{E}^{(4)}(\mathbf{r}) \cdot \mathbf{J}^{(2)}(\mathbf{r})dV = \int_{flaw} \mathbf{E}^{(2)}(\mathbf{r}) \cdot \mathbf{J}^{(4)}(\mathbf{r})dV, \qquad (53)$$

where the right hand side of (53) is the integral over the flaw of the dot product of the field, $\mathbf{E}^{(2)}(\mathbf{r})$, at the flaw due to the pickup current with the current density, $\mathbf{J}^{(4)}(\mathbf{r})$, of the flaw current. This symmetry is reflected in the coefficients of I_4 and I_2 in (45) and (49) respectively, which are equal as are the Z_{ij} under the interchange of i and j.

With this equality we can now write the change in the transfer impedance due to the flaw as:

$$dZ_{21} = \frac{dV_2}{I_1} = \frac{-\int_{flaw} \mathbf{E}^{(2)}(\mathbf{r}) \cdot \mathbf{J}^{(4)}(\mathbf{r})dV}{I_2(1)I_1}. \qquad (54)$$

The current $\mathbf{J}^{(4)}(\mathbf{r})$ is the flaw current due to the driver current, and is therefore proportional to I_1. The field $\mathbf{E}^{(2)}(\mathbf{r})$is the field at the flaw due to the pickup current, and is therefore proportional to $I_2(1)$. From the second term of (49), it's clear that $\mathbf{E}^{(2)}(\mathbf{r})$ includes the field at the flaw generated by the action of the pickup current on the background. And from (37) it's clear that it's computation includes the contributions of the ferrite core as well.

Thus, we can write the change in impedance due to the flaw as:

$$dZ_{21} = -\int_{flaw} \mathbf{E}^{(2)}(\mathbf{r}) \cdot \mathbf{J}^{(4)}(\mathbf{r})dV = \sum_{KLM} E^{(x)}_{KLM} J^{(x)}_{KLM} + E^{(y)}_{KLM} J^{(y)}_{KLM} + E^{(z)}_{KLM} J^{(z)}_{KLM}, \qquad (55)$$

where in the last expression the sum is over the x, y, and z indices, K, L, and M of the flaw grid, J is the solution $\mathbf{J}_f$ obtained in solving (28) for a driver coil current of unity, and E is given by the right-hand side of that equation, where $\mathbf{M}_c$ and $\mathbf{J}_b$ are the solutions obtained in solving (26) and (27) for a pickup coil current of unity.

V. COMMENTS AND CONCLUSIONS

We have developed a model for computing solutions to multiscale problems based on coupled integral equations, and have reduced the equations to matrix form using the usual techniques of the method of moments. We have shown, further, that the development of the model equations and the interpretation of the model results is facilitated by the use of classical electrical equivalent circuits. This is one of the advantages in choosing electrical impedance to be the observable in the solution of the field equations.

The algorithm developed in this paper is being coded into the commercial product, **VIC-3D®**. In future papers, we will describe its application to a number of problems in aircraft inspection, as well as discuss our success with such coding concerns as parallelization and the use of GPU hardware.

ACKNOWLEDGEMENT

This work was supported by the Air Force Research Laboratory under SBIR contract FA8650-13-C-5011 with Victor Technologies, LLC.

REFERENCES

[1] H. A. Sabbagh, R. K. Murphy, E. H. Sabbagh, J. C. Aldrin, and J. S. Knopp, *Computational Electromagnetics and Model-Based Inversion: A Modern Paradigm for Eddy-Current Nondestructive Evaluation*, Springer, New York, 2013.

R. Kim Murphy received his B.A. in Physics from Rice University in 1978, and his Ph.D. in Physics from Duke University in 1984. Since 1989, he has worked as a Senior Physicist for Sabbagh Associates Inc., and Victor Technologies, LLC. Murphy has been active in formulating models and coding in VIC-3D, performing validation numerical experiments, and solving one-dimensional and three-dimensional inverse problems.

Harold A. Sabbagh received his BSEE and MSEE from Purdue University in 1958, and his Ph.D. from Purdue in 1964. In 1980, he formed Sabbagh Associates, Inc., and did research in the application of computational electromagnetics to nondestructive evaluation (NDE). This research evolved into the commercial volume-integral code, VIC-3D. In 1998, he formed Victor Technologies, LLC, in order to continue this research and further development of VIC-3D. His past professional activities have included a stint as President of ACES, and in 2010, he was elected to the grade of Fellow in ACES.

Elias H. Sabbagh received the B.Sc. in Electrical Engineering and the B.Sc. in Economics from Purdue University in 1990 and 1991. He has worked as System Administrator, Software Engineer, and Researcher for Victor Technologies since its inception. His interests include object-oriented programming, database administration, system architecture, scientific programming, and distributed programming.